

# Relationship Between Glenoid Deformity and Gait Characteristics in a Rat Model of Neonatal Brachial Plexus Injury

Kelsey Hennen,<sup>1</sup> Dustin L. Crouch,<sup>2</sup> Ian D. Hutchinson,<sup>3</sup> Zhongyu Li,<sup>3</sup> Katherine Saul<sup>1</sup>

<sup>1</sup>Department of Mechanical and Aerospace Engineering, North Carolina State University, Raleigh, North Carolina, <sup>2</sup>Department of Mechanical, Aerospace, and Biomedical Engineering, The University of Tennessee, Knoxville, Tennessee, <sup>3</sup>Department of Orthopaedic Surgery, Wake Forest School of Medicine, Winston-Salem, North Carolina

Received 31 May 2017; accepted 4 December 2017

Published online 15 December 2017 in Wiley Online Library (wileyonlinelibrary.com). DOI 10.1002/jor.23836

**ABSTRACT:** Neonatal brachial plexus injury (NBPI) results in substantial postural and functional impairments associated with underlying muscular and osseous deformities. We examined the relationship between glenoid deformity severity and gait in a rat model of NBPI, an established model for studying the in vivo pathomechanics of NBPI. At 8 weeks post-operatively, we monitored the gait of 24 rat pups who exhibited varying degrees of glenoid deformity following unilateral brachial plexus neurectomy and chemodenervation interventions administered 5 days postnatal. Five basic stride and stance metrics were calculated for the impaired forelimbs over four consecutive gait cycles. Bilateral differences in glenoid version ( $\Delta GA_v$ ) and inclination ( $\Delta GA_i$ ) angles were computed from data for the same rats as reported in a previous study. A linear regression model was generated for each deformity-gait pair to identify significant relationships between the two.  $\Delta GA_v$  was not significantly correlated with any gait measurements, while  $\Delta GA_i$  significantly correlated with all five gait measurements. Specifically,  $\Delta GA_i$  was significantly positively correlated with stride length ( $R^2 = 0.38$ ,  $p = 0.001$ ) and stance factor ( $R^2 = 0.45$ ,  $p < 0.001$ ), and significantly negatively correlated with stance width ( $R^2 = 0.24$ ,  $p = 0.016$ ), swing/stance ratio ( $R^2 = 0.17$ ,  $p = 0.046$ ), and stride frequency ( $R^2 = 0.33$ ,  $p = 0.003$ ). Rats with declined glenoids exhibited the most altered gait. Clinical significance: Our findings link musculoskeletal changes and functional outcomes in an NBPI rat model. Thus, gait analysis is a potentially useful, non-invasive, quantitative way to investigate the effects of injury and deformity on limb function in the NBPI rat model. © 2017 Orthopaedic Research Society. Published by Wiley Periodicals, Inc. *J Orthop Res* 36:1991–1997, 2018.

**Keywords:** gait; shoulder; animal model; brachial plexus; deformity

Neonatal brachial plexus injury (NBPI), primarily affecting cervical roots C5 through C8,<sup>1,2</sup> occurs in 0.42–5.1 of every 1,000 live births via the birth canal<sup>3–5</sup> and 0.2–2.0 of every 1,000 births via Caesarean section.<sup>6</sup> Estimates of incomplete neurological recovery range widely,<sup>7</sup> but were reported to be as high as 27% in one prospective large-scale study.<sup>5</sup> Infants without full neurological recovery predominantly display glenoid retroversion,<sup>8,9</sup> which may also be accompanied by posterior humeral head subluxation,<sup>10</sup> malformation of the humeral head and glenoid,<sup>8,10</sup> and glenoid declination.<sup>9,11,12</sup> Rotator cuff muscular imbalance and internal rotation contracture<sup>4,10</sup> is also attributed to NBPI, with associated subscapularis shortening and stiffening,<sup>13</sup> and weakening or paralysis of the infraspinatus and supraspinatus.<sup>14</sup> Although quantitative data collection from infants and children is limited in the literature, it is known that NBPI patients have overall reduced passive and active range of motion that is correlated with deformity.<sup>15,16</sup> The most significant range of motion restriction is seen for passive movement,<sup>17</sup> with horizontal adduction, shoulder adduction, and external rotation most negatively affected.<sup>4</sup> Children with NBPI also experience motor and sensory deficits that are associated with relatively poor performance of activities of daily living.<sup>18</sup>

Animal models are often used to elucidate the mechanisms of deformity and loss of function following brachial plexus injury.<sup>19–24</sup> Since humans and rodent animal models share similar shoulder joint anatomy and innervation of the brachial plexus,<sup>23</sup> rat models are commonly used. Surgical infliction of brachial plexus injury in rats 5 days postnatal results in gross musculoskeletal and postural deformities that reflect patterns observed in human patients,<sup>24</sup> as described by several groups.<sup>19–21,24</sup> Specifically, based on non-invasive micro-CT imaging, rat models of NBPI exhibit shoulder dislocation,<sup>19–21</sup> decreased humeral head size,<sup>20,21,24</sup> flattening of the humeral head,<sup>20</sup> glenoid retroversion,<sup>19,21</sup> and glenoid declination.<sup>19,20</sup> Muscle changes that have been seen in the NBPI rat model include subscapularis and infraspinatus muscle atrophy<sup>24</sup> and shortening of the pectoralis major, supraspinatus, and subscapularis.<sup>19</sup>

While the extent of bone and muscle alterations following injury in the NBPI rat model has been well characterized, it remains unclear how the degree of deformity relates to functional limitations. The previous quantitative methods, including non-invasive imaging under sedation or post-mortem imaging and dissection, only assess the severity of shoulder deformation, not the relationship to active limb function. These assessment procedures are also relatively challenging to perform and limit the information that could be obtained in longitudinal studies of injury progression. Post-injury passive range of motion has been recorded in animal models of NBPI under sedation and post-mortem,<sup>19–21,24</sup> as well as qualitative descriptions of rat gait following NBPI.<sup>23</sup> However, the quantitative effect of NBPI in the rat model

Grant sponsor: Pediatric Orthopaedic Society of North America; Grant sponsor: Orthopaedic Research and Education Foundation.

Correspondence to: Katherine R. Saul (T: 919-515-1273; F: 919-515-7968; E-mail: ksaul@ncsu.edu)

© 2017 Orthopaedic Research Society. Published by Wiley Periodicals, Inc.

on active function and the relationship between osseous deformity and active function have not been previously studied.

Given that clinical studies have shown clear relationships between osseous deformity and limb function,<sup>15,16</sup> we expected that the same would be true in a NBPI rat model. If so, gait analysis would potentially be a useful non-invasive *function-based* quantitative method for monitoring both the progression of injury and efficacy of novel treatment strategies in the NPBI rat model. Therefore, we quantified differences in gait function in a rat model of NBPI and conducted a retrospective analysis to examine the relationship between osseous deformity severity and functional changes to gait in rats with a brachial plexus injury. Specifically, we focused on the effect of glenoid version and glenoid inclination on gait, since glenoid deformity is a hallmark of clinical NBPI.<sup>15,16</sup> We hypothesized that gait would be altered following NBPI, and that rats with more severe glenoid deformity would exhibit greater adverse changes in gait.

**METHODS**

The following procedures were approved by the Institutional Animal Care and Use Committee. As part of a previous study to elucidate the role of muscle changes on osseous deformity,<sup>19</sup> 32 5-day-old Sprague Dawley rat pups (Harlan Laboratories, Indianapolis, IN) underwent surgical intervention on the left forelimb while anesthetized with inhalative isoflurane. Details of the interventions are available in the prior publication.<sup>19</sup> Briefly, rat pups received interventions including neurectomy of the brachial plexus upper trunk, botulinum neurotoxin A (Botox) injections, a combination of the two, or a sham surgery. The contralateral limb in all animals was also maintained as additional control.

In the prior report, measurements of glenoid version angle and glenoid inclination angle were made from 3D-reconstructed micro-CT images.<sup>19</sup> The images were acquired post-sacrifice at 8 weeks post-intervention. Glenoid version angle ( $GA_v$ ), measured in the plane of the scapular spine, was  $90^\circ$  minus the posteromedial angle between two lines: (i) a line from the medial aspect of the scapula through the center of the glenoid, and (ii) a line connecting the anterior and posterior margins of the glenoid fossa<sup>16</sup> (Fig. 1).

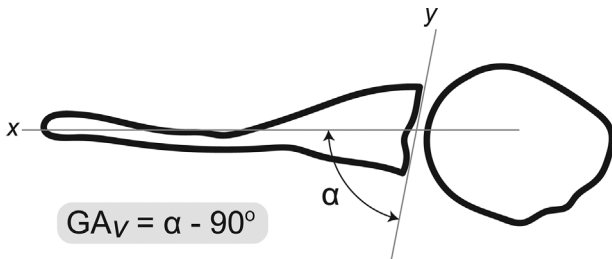


**Figure 1.** Glenoid version definition. Glenoid version angle ( $GA_v$ ), measured in the plane of the scapular spine, was defined as  $\alpha - 90^\circ$ , where  $\alpha$  is the angle between a line from the medial aspect of the scapula and through the glenoid (line  $x$ ) and the line tangent to the rim of the glenoid fossa (line  $y$ ). The glenoid is considered more retroverted as  $\alpha$  decreases and anteverted as  $\alpha$  increases.

Glenoid inclination angle ( $GA_i$ ) was defined as the angle between the scapular spine centerline and the line tangent to the glenoid fossa rim, minus  $90^\circ$ , as measured in the subscapular fossa plane<sup>19</sup> (Fig. 2).

To quantify the degree of symmetry in glenoid version and inclination between the left and right shoulders, the difference in glenoid angle between the affected and unaffected shoulders were calculated for each rat (Equation 1).

$$Glenoid\ Angle\ Difference = \Delta GA = GA_{affected} - GA_{unaffected} \tag{1}$$

**Gait Analysis**

At 8 weeks post-operatively, the gait of each rat was monitored while walking on a treadmill (DigiGait Imaging System, Quincy, MA) set to a constant speed of 10 cm per second with no incline.<sup>25,26</sup> Trials were continued or repeated until each rat walked for four consecutive gait cycles. For 17 rats, only one trial was conducted; for seven rats, two or three trials were necessary to obtain four consecutive gait cycles. We were unable to collect a sufficient number of gait data for eight rats due to non-compliance. Thus, data from 24 of the 32 rats were included in subsequent analysis. Stride length, stride frequency, stance factor, stance width, and swing to stance ratio were calculated for the impaired forelimbs using the camera underneath the treadmill belt (Fig. 3); contact location was calculated as the centroid of the contact area. Stride length is the total distance the impaired limb travels over one step. Stride frequency is the number of steps per second. Stance factor is the ratio between average stance durations of the impaired and unaffected forelimbs; a stance factor of 1 represents symmetric gait. Stance width is the measured distance between the centroids of the forelimb contact areas. The swing to stance ratio is the ratio between the average swing and stance durations of the impaired limb.

**Data Analysis**

A linear regression model was fit for each pair of  $\Delta GA$  and gait characteristic across groups to identify potential relationships between observed glenoid deformity and gait impairment. Four samples (one from neurectomy intervention group, three from neurectomy and chemodenervation intervention group)

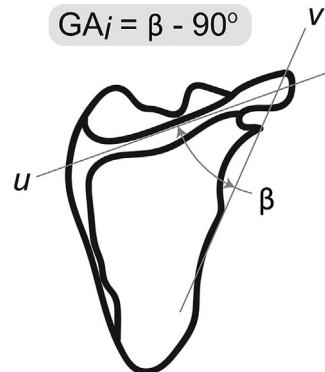


**Figure 2.** Glenoid inclination definition. Glenoid inclination angle ( $GA_i$ ), measured in the plane of the subscapular fossa, was defined as  $\beta - 90^\circ$ , where  $\beta$  is the angle between the centerline of the scapular spine (line  $u$ ) and the line tangent to the rim of the glenoid fossa (line  $v$ ). The glenoid is considered more declined as  $\alpha$  decreases and inclined as  $\alpha$  increases.

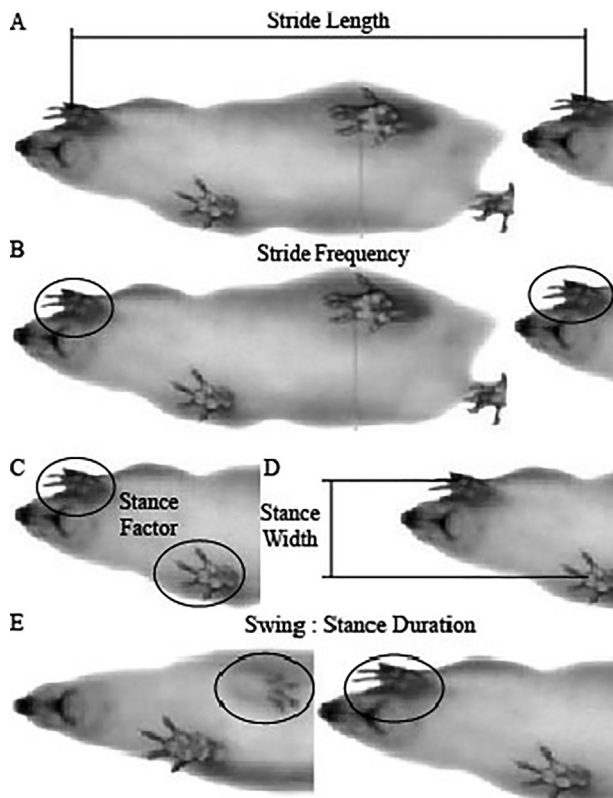


**Figure 3.** Quadrupedal gait characteristics. (A) Stride length is the distance the centroid of the impaired forelimb travels in one stride. (B) Stride frequency was calculated as the number of strides/sec of the impaired limb. (C) Stance factor is the ratio of stance duration of the impaired and unimpaired forelimbs. (D) Stance width was defined as the orthogonal distance between the centroids of the forepaws at peak stance. (E) Swing: Stance is the ratio between swing and stance durations of the impaired limb<sup>22</sup>.

were excluded from the  $\Delta GA_v$  regression analysis because they were determined to be outliers based on a quantile-quantile plot test for normality of  $\Delta GA_v$ . Regression coefficients were considered significant for  $\alpha \leq 0.05$ . Given the pilot nature of this study, no adjustment was made for multiple comparisons.

## RESULTS

Linear regression analysis indicated that  $\Delta GA_v$  tended to be correlated with stance width ( $R^2=0.19$ ,  $p=0.056$ ) (Fig. 4). However, there was no significant linear relationship between  $\Delta GA_v$  and stride length ( $R^2=0.038$ ,  $p=0.411$ ), stance factor ( $R^2=0.009$ ,  $p=0.685$ ), swing/stance ratio ( $R^2=9.9 \times 10^{-5}$ ,  $p=0.967$ ), and stride frequency ( $R^2=0.12$ ,  $p=0.140$ ).

All five gait performance metrics were statistically significantly related to  $\Delta GA_i$  (Fig. 5). Specifically,  $\Delta GA_i$  was significantly correlated with stance width ( $R^2=0.24$ ,  $p=0.016$ ), stride length ( $R^2=0.38$ ,  $p=0.001$ ), stance factor ( $R^2=0.45$ ,  $p<0.001$ ), swing/stance ratio ( $R^2=0.17$ ,  $p=0.046$ ), and stride frequency ( $R^2=0.33$ ,  $p=0.003$ ).

Linear regression models revealed how gait characteristics varied with glenoid inclination angle deformity severity, as indicated by  $\Delta GA_i$  (Fig. 5). For

instance, rats with declined glenoids took shorter steps and had a higher stride frequency than those with higher glenoid inclination angles. Stance metrics also indicated that rats with declined glenoids had higher forelimb stance width and lower stance factor. Rats with declined glenoids had higher swing/stance ratios, indicating that they spent less time in stance on the affected limb than rats with higher glenoid inclination angles. Of the eight rats with the most declined glenoid, seven walked on the elbow of the affected limb instead of the paw, while one rat did not place any part of the affected limb on the treadmill.

## DISCUSSION

We quantitatively evaluated the gait of rats with NBPI, and found that variation in glenoid inclination angle deformity, as quantified by  $\Delta GA_i$ , was significantly correlated with altered gait characteristics in the impaired limb, while  $\Delta GA_v$  was not. Rats with a declined glenoid exhibited the most severe gait changes. Our results are consistent with another prior qualitative experiment in which gait was studied in a NBPI rat model.<sup>23</sup> Using a paper runway on which the rats walked at their self-selected speed, Ochiai et al. divided the rats into three groups based on how the impaired limb was used during gait. Rats were given a low clinical score when walking on all four paws normally, a medium clinical score when the impaired limb trailed slightly behind the unaffected limb, and a high clinical score when the impaired limb was dragged across the floor. When required to walk on a horizontal grid, rats with the worst clinical scores also exhibited decreased stability, frequently misplacing the impaired limb and falling through the grid.<sup>23</sup> While these results are consistent with the current study in which we also observed altered gait, Ochiai et al.<sup>23</sup> study was unable to provide quantitative gait metrics, and did not provide information regarding the underlying degree of osseous or muscular abnormality. In addition, the inflicted neurectomy of the brachial plexus was preganglionic in that study, while the current study employed a postganglionic model of NBPI. Nikolaou et al.<sup>22</sup> reported that preganglionic neurectomy preserves muscle spindles during development and exhibited reduced internal rotation contracture, while postganglionic neurectomy was associated with more severe contracture and disorganized spindle structure. Therefore, gait characteristics between the two types of NBPI may differ.

While our regression analysis identified a statistically significant relationship between glenoid deformity and gait characteristics, the underlying cause of gait adaptations remains unclear. One confounding factor among animals was that some walked on their elbows of the affected forelimb, while others walked on their paws. Post-intervention musculoskeletal changes

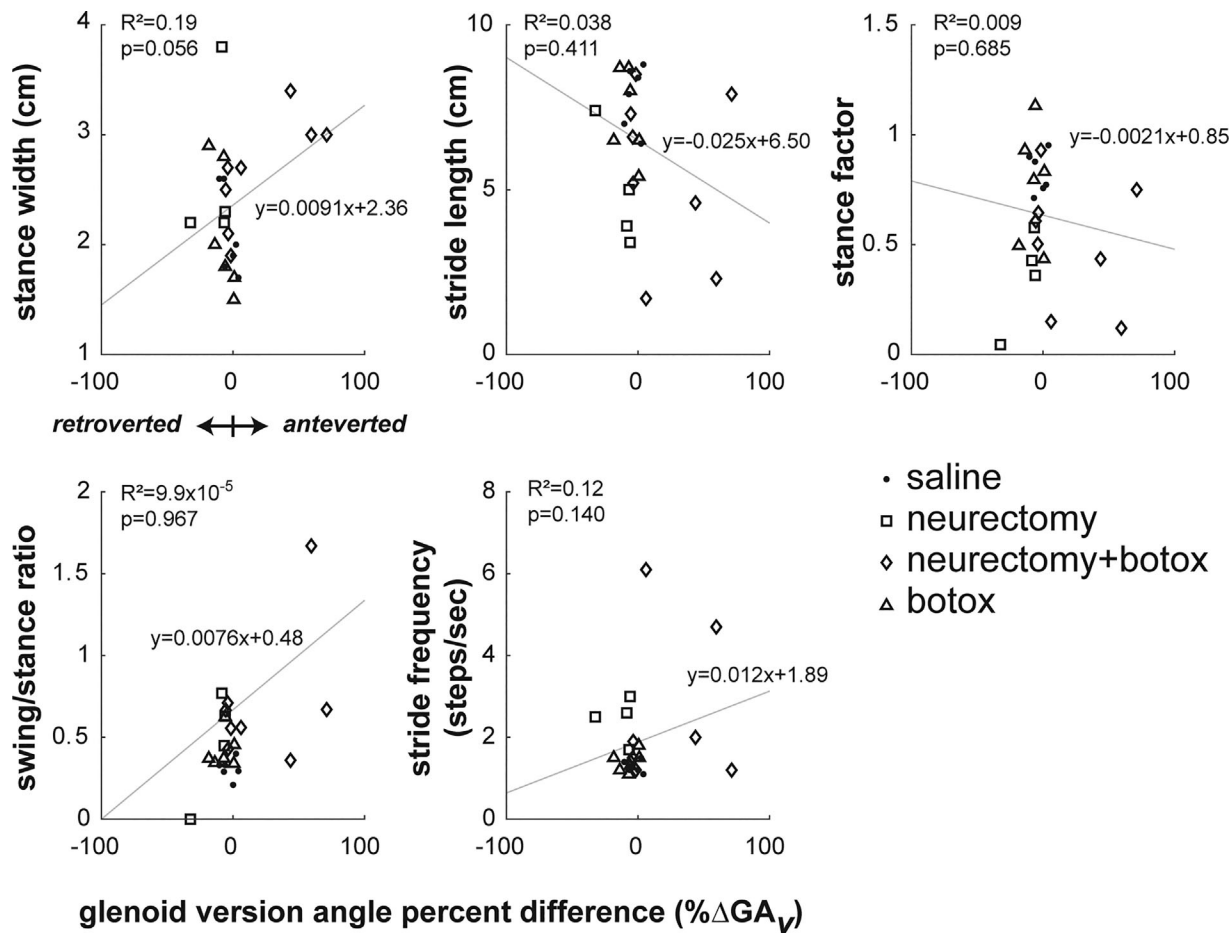


**Figure 4.** Linear regression between glenoid version angle difference ( $\Delta GA_v$ ) and gait characteristics. Equations are given for each regression line (gray line), as well as  $R^2$  and  $p$ -values for each regression. None of the regression slope coefficients were significantly different from zero.

in the animals may have also contributed to the observed gait differences among animals. For instance, musculoskeletal changes were suspected to have reduced external rotation range of motion, as measured following neurectomy in the group of animals studied here.<sup>19</sup> Muscles were also likely weak or paralyzed following neurectomy. Optimal muscle fiber lengths of the pectoralis major, supraspinatus, and subscapularis were shortened, and cross-sectional areas of all rotator cuff muscles decreased in animals that underwent neurectomy.<sup>19</sup> Other clinically observed factors that potentially altered gait include injury-induced sensory impairment<sup>27</sup> and changes in limb segment lengths.<sup>28</sup>

As discussed in the previous paragraph, it is likely that a combination of neuromuscular and skeletal morphology changes contributed to the observed gait differences. Simulation using animal and computational models could help identify the relative contribution of each factor to impairment independently, and reveal factors that may be effective targets for clinical intervention. For instance, the effect of elbow walking on gait could be determined by comparing gait characteristics between rats with and without elbow disarticulation. Aspects of the glenoid deformity, such as

retroversion, could be created by surgical or mechanical intervention to study the effects of deformity apart from muscle changes. Conversely, creating a brachial plexus injury in older rats may induce, and highlight the effects of, muscle changes without bone deformity.

Although the animals in the current study were divided among surgical groups for the purposes of the prior report, we combined animals together across all surgical groups to perform the regression analysis, rather than compare among groups. Not all rats in each surgical group exhibited severe musculoskeletal changes,<sup>19</sup> possibly due to variation in the administration of and animals' response to the surgical and chemodenervation interventions. Additionally, some animals may have experienced spontaneous neurological recovery, as is observed in human NBPI patients in up to 50% of cases within 3 months and 82% within 18 months from birth.<sup>18</sup> Given high within-group variability in post-intervention outcomes, gait differences between intervention groups were not as marked. However, note that rats exhibiting a declined glenoid had undergone a neurectomy, which was previously associated with more severe osseous and

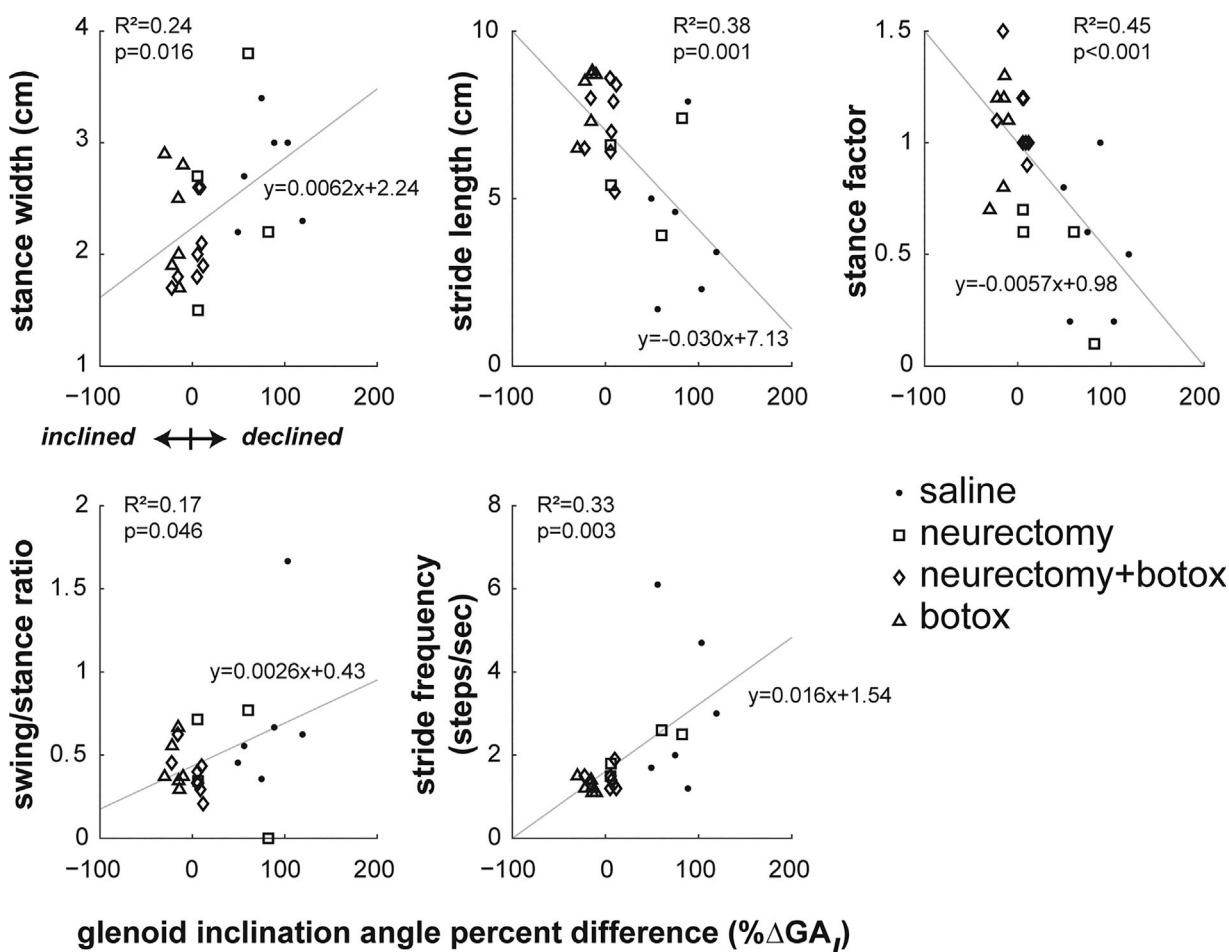


**Figure 5.** Linear regression between glenoid inclination angle difference ( $\Delta GA_i$ ) and gait characteristics. Equations are given for each regression line (gray line), as well as  $R^2$  and  $p$ -values for each regression. All regression slope coefficients were significantly different from zero.

muscular changes compared to chemodenervation alone.<sup>19</sup>

Animal models of NBPI are important and useful tools for investigating clinical pathology in a more comprehensive and controlled manner than is practical or possible in humans. However, as with all models, it is important to carefully consider differences between the NBPI rat model and clinical scenario when comparing the two. In humans, glenoid retroversion, not glenoid declination, is considered the prominent, classic glenoid deformity characteristic in children with NBPI.<sup>15,16</sup> We hypothesize that  $\Delta GA_i$  was more strongly associated with gait characteristics than  $\Delta GA_v$  in the rat model because forelimb humeral motion during quadrupedal gait primarily occurs in the superoinferior direction, which is the same approximate direction of glenoid inclination angle changes. Though glenoid version angle is the most common clinical measure of glenoid deformity in NBPI, glenoid deformity may not be limited to the axial plane. Two recent studies that evaluated the three-dimensional morphology of the glenoid found that the glenoid on the affected side was significantly more retroverted

and declined in children with NBPI.<sup>11,12</sup> Another study found that glenoid retroversion deformity severity was negatively correlated with glenoid declination deformity severity.<sup>9</sup> Though the relationship between glenoid retroversion and function is well established,<sup>15,16</sup> the possible pattern of glenoid declination and its effect on function must be investigated further. In addition, the active functional outcome examined here is quadrupedal and not typical of human upper limb movement, limiting direct clinical relevance. However, within the context of the animal model, understanding the active functional repercussions of structural changes in addition to passive outcomes such as range of motion is critical to comprehensively evaluate the effects of NBPI.

There were several limitations of our study. First, despite similar observations of muscular and osseous changes between our rat model and infants with NBPI, there are major differences between rats and humans that warrant caution when translating our findings directly to clinical cases. For instance, rats are quadrupedal while humans are so for only about 1 year, leading to differences in biomechanical shoul-

der loading that may affect deformity progression. The tested sample size of rats was relatively small, so some gait differences were possibly undetected. The number of animals included in the analysis was based on the sample size of a previous study.<sup>19</sup> Eight of the 32 rats from the previous study were not included in the data analysis because we were unable to collect gait data over a sufficient number of strides. Of the eight excluded rats, 1, 2, and 5 of the rats exhibited glenoid inclination angles on the affected side that were declined, typical, and inclined, respectively, based on  $\Delta GA_i$ . Since we observed the most prominent gait alterations in rats with declined glenoids, other factors (e.g., animal reluctance to walk), rather than excessive functional impairment, likely explain why we were unable to collect sufficient data from the excluded animals. Chemodenervation was used in two surgical intervention groups to elicit specific biomechanical conditions in the rat model; however, chemodenervation effects can be widespread and may have affected more tissues than the intended muscular targets. Finally, the eight rats with the most severe glenoid declination did not walk on the paws of the affected limbs, which likely conflated with the effects of shoulder deformity on gait measurements.

We conclude that the severity of glenoid inclination angle deformity, particularly in rats with a declined glenoid, was significantly associated with altered gait, while glenoid version angle was not. This work supports the use of gait analysis as a non-invasive, quantitative functional assessment tool, and potential indicator of shoulder deformity severity in the NBPI rat model. As the mechanism of deformity following NBPI and potential treatments continue to be investigated, quantitative gait analysis is potentially valuable for monitoring progression of injury, recovery, or the effectiveness of treatments in longitudinal studies.

#### AUTHORS' CONTRIBUTIONS

KH performed data analysis, drafted the paper, approved the paper for submission. DC co-developed the study design, collected data, critically revised the paper, approved the paper for submission. IH executed the animal surgical procedures, critically reviewed the paper, approved the paper for submission. ZL co-developed the study design, approved the paper for submission. KS co-developed the study design, drafted the paper, approved the paper for submission. All authors have read and approved the final submitted manuscript.

#### REFERENCES

- Hogendoorn S, van Overvest KL, Watt I, et al. 2010. Structural changes in muscle and glenohumeral joint deformity in neonatal brachial plexus palsy. *J Bone Joint Surg Am* 92:935–942.
- Lagerkvist AL, Johansson U, Johansson A, et al. 2010. Obstetric brachial plexus palsy: a prospective, population-based study of incidence, recovery, and residual impairment at 18 months of age. *Dev Med Child Neurol* 52:529–534.
- Evans-Jones G, Kay SP, Weindling AM, et al. 2003. Congenital brachial palsy: incidence, causes, and outcome in the United Kingdom and Republic of Ireland. *Arch Dis Child Fetal Neonatal Ed* 88:F185–F189.
- Hoeksma AF, Ter Steeg AM, Dijkstra P, et al. 2003. Shoulder contracture and osseous deformity in obstetrical brachial plexus injuries. *J Bone Joint Surg Am* 85-A:316–322.
- Hoeksma AF, Wolf H, Oei SL. 2000. Obstetrical brachial plexus injuries: incidence, natural course and shoulder contracture. *Clin Rehabil* 14:523–526.
- Foad SL, Mehlman CT, Ying J. 2008. The epidemiology of neonatal brachial plexus palsy in the United States. *J Bone Joint Surg Am* 90:1258–1264.
- Pondaag W, Malessy MJ, van Dijk JG, et al. 2004. Natural history of obstetric brachial plexus palsy: a systematic review. *Dev Med Child Neurol* 46:138–144.
- Eismann EA, Little KJ, Laor T, et al. 2015. Glenohumeral abduction contracture in children with unresolved neonatal brachial plexus palsy. *J Bone Joint Surg Am* 97:112–118.
- Eismann EA, Laor T, Cornwall R. 2016. Three-dimensional magnetic resonance imaging of glenohumeral dysplasia in neonatal brachial plexus palsy. *J Bone Joint Surg Am* 98:142–151.
- van Gelein Vitringa VM, van Kooten EO, Jaspers RT, et al. 2009. An MRI study on the relations between muscle atrophy, shoulder function and glenohumeral deformity in shoulders of children with obstetric brachial plexus injury. *J Brachial Plex Peripher Nerve Inj* 4:9.
- Brochard S, Mozingo JD, Alter KE, et al. 2016. Three dimensionality of gleno-humeral deformities in obstetrical brachial plexus palsy. *J Orthop Res* 34:675–682.
- Frich LH, Schmidt PH, Torfing T. 2017. Glenoid morphology in obstetrical brachial plexus lesion: a three-dimensional computed tomography study. *J Shoulder Elbow Surg* 26:1374–1382.
- Einarsson F, Hultgren T, Ljung BO, et al. 2008. Subscapularis muscle mechanics in children with obstetric brachial plexus palsy. *J Hand Surg Eur Vol* 33:507–512.
- Birch R. 2002. Obstetric brachial plexus palsy. *J Hand Surg Br*. 27:3–8.
- Kozin SH. 2004. Correlation between external rotation of the glenohumeral joint and deformity after brachial plexus birth palsy. *J Pediatr Orthop* 24:189–193.
- Waters PM, Smith GR, Jaramillo D. 1998. Glenohumeral deformity secondary to brachial plexus birth palsy. *J Bone Joint Surg Am* 80:668–677.
- Pearl ML. 2009. Shoulder problems in children with brachial plexus birth palsy: evaluation and management. *J Am Acad Orthop Surg* 17:242–254.
- Sundholm LK, Eliasson AC, Forsberg H. 1998. Obstetric brachial plexus injuries: assessment protocol and functional outcome at age 5 years. *Dev Med Child Neurol* 40:4–11.
- Crouch DL, Hutchinson ID, Plate JF, et al. 2015. Biomechanical basis of shoulder osseous deformity and contracture in a rat model of brachial plexus birth palsy. *J Bone Joint Surg Am* 97:1264–1271.
- Li Z, Ma J, Apel P, et al. 2008. Brachial plexus birth palsy-associated shoulder deformity: a rat model study. *J Hand Surg Am* 33:308–312.
- Li Z, Barnwell J, Tan J, et al. 2010. Microcomputed tomography characterization of shoulder osseous deformity

- after brachial plexus birth palsy: a rat model study. *J Bone Joint Surg Am* 92:2583–2588.
22. Nikolaou S, Hu L, Cornwall R. 2015. Afferent innervation, muscle spindles, and contractures following neonatal brachial plexus injury in a mouse model. *J Hand Surg Am* 40:2007–2016.
  23. Ochiai H, Ikeda T, Mishima K, et al. 2002. Development of a novel experimental rat model for neonatal pre-ganglionic upper brachial plexus injury. *J Neurosci Methods* 119:51–57.
  24. Soldado F, Benito-Castillo D, Fontecha CG, et al. 2012. Muscular and glenohumeral changes in the shoulder after brachial plexus birth palsy: an MRI study in a rat model. *J Brachial Plex Peripher Nerve Inj* 7:9.
  25. Eftaxiopoulou T, Macdonald W, Britzman D, et al. 2014. Gait compensations in rats after a temporary nerve palsy quantified using temporo-spatial and kinematic parameters. *J Neurosci Methods* 232:16–23.
  26. Hansen ST, Pulst SM. 2013. Response to ethanol induced ataxia between C57BL/6J and 129 × 1/SvJ mouse strains using a treadmill based assay. *Pharmacol Biochem Behav* 103:582–588.
  27. Anand P, Birch R. 2002. Restoration of sensory function and lack of long-term chronic pain syndromes after brachial plexus injury in human neonates. *Brain* 125:113–122.
  28. McDaid PJ, Kozin SH, Thoder JJ, et al. 2002. Upper extremity limb-length discrepancy in brachial plexus palsy. *J Pediatr Orthop* 22:364–366.